Salient Object Detection via Color Contrast and Color Distribution

Keren Fu, Chen Gong, Jie Yang, and Yue Zhou

Institute of Image Processing and Pattern Recognition,
Shanghai Jiao Tong University, and Key Laboratory of System Control and Information Processing, Ministry of Education of China, Shanghai 200240

Abstract. In this paper, we take the advantages of color contrast and color distribution to get high quality saliency maps. The overall procedure flow of our unified framework contains superpixel pre-segmentation, color contrast and color distribution computation, combination, final refinement and then object segmentation. During color contrast saliency computation, we combine two color systems and then introduce the using of distribution prior before saliency smoothing. It works to select correct color components. In addition, we propose a novel saliency smoothing procedure that is based on superpixel regions and is realized in color space. This processing step leads to total object being highlighted evenly, contributing to high quality color contrast saliency maps. Finally, a new refinement approach is utilized to eliminate artifacts and recover unconnected parts in the combined saliency maps. In visual comparison, our method produces higher quality saliency maps which stress out the total object meanwhile suppress background clutters. Both qualitative and quantitative experiments show our approach outperforms 8 state-of-the-art methods, achieving the highest precision rate 96% (3% improvement from the current highest), when evaluated via one of the most popular data sets [1]. Excellent content-aware image resizing also can be achieved with our saliency maps.

1 Introduction

Human usually pay more attention to some parts of a given image. This visual attention mechanism has been extensively studied by researchers, due to it can allow us to allocate our sensory and computational resources to the most valuable information. Salient object detection is one of the most important aspects of such attention mechanism. Various applications have been explored by using saliency detection, such as auto target location and segmentation [2, 3], object based image retrieval [4], content-aware image resizing [5–8] and so on.

Saliency models usually can be divided into two categories, so-called *bottom-up* and *top-down*. Bottom-up model [9–13, 1, 14] simulates our instinctive visual attention mechanism and lots of low-level features like color (intensity), edge (texture) could be adopted. A salient object should be unique or have strong contrast compared to its surroundings on theses features. Among them, color contrast is one low-level feature which may easily draw our attention [15, 16].

K.M. Lee et al. (Eds.): ACCV 2012, Part I, LNCS 7724, pp. 111–122, 2013.

Another model called top-down [17–19] is defined in visual perceptual field as using effective memory to process presented saliency information. Via the computer vision techniques, we can realize the top-down model through combining the prior statistical knowledge and learning of classifiers.

In this paper, we take the advantages of color contrast and color distribution to carry out our saliency detection, so our method belongs to bottom-up kind. The previous work which is most related to ours is [10] and recent [11]. The former defines pixel-wise saliency as a pixel's contrast to all other pixels. This is then converted into computation based on color histogram. Also, good results are reported using HC (Histogram Contrast) and RC (Region Contrast) methods in [10]. However, we find that their methods only consider the color contrast but exclude the color distribution, which may also be an important kind of character for salient object. So their HC and RC methods may not get good results on the images in which some parts of background have relatively stronger contrast than the real salient object. Besides, the saliency maps obtained using RC usually highlights some parts of salient object, rather than the overall, and there are also lots of background clutters, as is shown in Fig.3 and Fig.4.

In addition, our work differs from [11] as we perform more processing steps in our color contrast based saliency computation, which are proved to be necessary to improve the final performance in a relative large margin. Moreover, we propose a different approach to refine our saliency maps.

In summary, we propose that a salient object should have the following characters on color feature, in two folds, the color contrast and color distribution.

(*i*). The color components belong to a salient object may have strong contrast to their surroundings, which is biologically inspired. (*contrast*)

(*ii*). These color components may be located near image center rather than image boundary. It is based on the fact [19] that shows human fixation has much higher probability to fall onto the center of image. (*distribution*)

(*iii*). These color components usually distribute compactly. In another word, color components which distribute widely are less likely to belong to a salient object. (*distribution*)

Our method takes the above three characters to perform saliency detection. The experimental results show our algorithm can highlight the whole part of a salient object meanwhile have strong ability to suppress background clutters. As a result, high quality saliency maps can be obtained.

The rest of this paper is organized as follows. Related works are described in Section 2. Our methodology is proposed in Section 3. Experimental results are analyzed in Section 4 while conclusion and future work are drawn in Section 5.

2 Related Work

As is mentioned above, the main categories of saliency detection methods are bottom-up and top-down. Because our method belongs to the former, here we only review related bottom-up kind. For top-down kind, we suggest readers to refer to [19].

Among bottom-up kind, as one of the earliest work, Itti *et al* [9] proposed a center-surround operation as local feature contrast in the color, intensity, and orientation of an image. The center-surround operation is realized using DOG (Difference of Gaussians). Then Hou *et al* [12] propose a method based on the spectral residual in the amplitude spectrum of Fourier transform. Zhai *et al* [13] define the saliency of each pixel as its contrast to all other pixels. However, for efficiency, they only consider the luminance channel. Achanta *et al* [1] propose a frequency tuned method which is extremely fast. They define the saliency of a pixel as its distance to the image average. But this algorithm is less promising for images that contain complex background and textures. Goferman *et al* [14] combine local feature and global feature to estimate the patch saliency in multi-scale. This leads to high computational cost. Besides, the use of local feature may cause edges highlighted. Cheng *et al* [10] propose Histogram Contrast based and Region Contrast based methods, called HC and RC respectively, as is mentioned in Section 1. Saliency maps obtained using their methods may contain background clutters and sometimes highlight parts of the object. Although they combine GrabCut [20] and their saliency maps to get good segmentation results, we demonstrate that high quality saliency map is the basis of various post processing. Thus the key point should be focused on how to improve the quality of the obtained saliency map. More recently, Perazzi *et al* [11] combine color contrast and color distribution to perform saliency detection. They show that the complete contrast and saliency estimation can be formulated in a unified way using high dimensional Gaussian filters. However, they only combine basic steps of computing color contrast and distribution.

Furthermore, there are some bottom-up methods which adopt multiple features. Liu *et al* [21] and Alexe *et al* [22] use a sliding window and compute a multiple low-level feature based saliency score for each window. Salient object corresponds to the window with the highest score. Feng *et al* [23] compute the window saliency based on superpixels. They use all the superpixels outside the window to compose the inside ones, thus the global image context is combined.

Our saliency detection method varies from the state-of-the-art bottom-up methods, because our method concentrates on how to produce high quality saliency maps which strongly highlight the total object as well as suppress the background clutters enormously. High quality saliency maps facilitate most post processing like object segmentation and content-aware image resizing, as we will show later.

3 Methodology

Fig.1 shows the whole procedure flow of our method, including SLIC superpixel pre-segmentation [24], color contrast and color distribution computation, combination, final refinement and then object segmentation. As high quality saliency maps are produced, using simple thresholding may achieve good segmentation results, as we will show in the final quantitative comparison. Note that an input image is first resized to the size of (W, H), which subjects to $\max(W, H) = 400$. Then all the parameters of our method are tuned on this basic resolution.

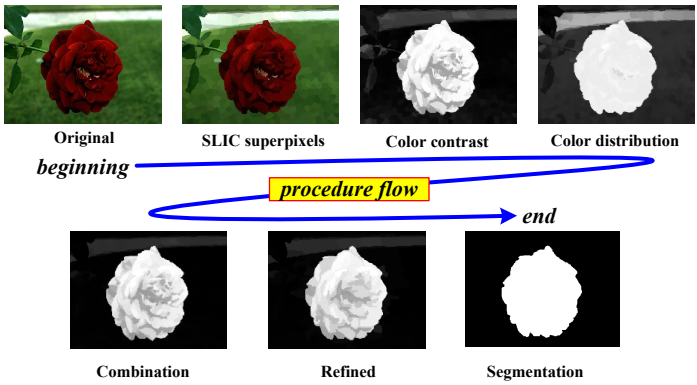

Fig. 1. The whole procedure flow of our method, including SLIC superpixel pre-segmentation, color contrast and color distribution computation, combination, final refinement and object segmentation

3.1 Pre-segmentation

In order to calculate color contrast of a pixel to all other pixels, a straightforward way is pixel-wise computation, as is mentioned in [13]. However, the computational cost of such algorithms is $O(M^2)$, where M denotes the number of pixels in the input image. An elegant way to speed up and reduce computational cost is histogram based computation [10, 13] or segmenting images into edge-preserving regions, like that in [10, 11, 23]. Pixels in the same region usually have homogenous color component. Computing region based contrast instead of pixel-wise operation enormously pulls down the computational complexity. Thus, we first use SLIC superpixels [24] to decompose an image and generate spatial compact regions $R_i, i = 1, 2, 3...N$. SLIC superpixels are also used in [11] as abstraction technique. Compact SLIC superpixels are generated iteratively using mean-shift clustering based on the initial uniformly distributed region seeds. We use SLIC superpixels in LAB color space, which well characterize human visual perception. For an image with basic resolution, we segment it into about $N = 500$ superpixels, a tradeoff between computational cost and description ability. Here we use c_i, p_i to denote the average color and position of superpixels as

$$c_i = \frac{\sum_{I_m \in R_i} I_m^C}{|R_i|}, \; p_i = \frac{\sum_{I_m \in R_i} I_m^P}{|R_i|} \tag{1}$$

where I_m^C and I_m^P are respectively 6D color vector, constituted by LAB and RGB components (corresponds c_i^{LAB} and c_i^{RGB}), and position vector of pixel I_m. $|R_i|$ is the sum area of superpixel region R_i. Pre-segmenting the image into superpixels eliminates unnecessary details and noises as well.

3.2 Color Contrast

According to character (i), we define region's color contrast saliency $S_i^{contrast}$ as

$$S_i^{contrast} = \sum_j D(c_i, c_j)^2 w_{ij}^P \tag{2}$$

in which $D(c_i, c_j) = ||c_i - c_j||_2$ is Euclidean distance between c_i and c_j. That means we first combine both color systems in color contrast computation. This is motivated by one color system does not always work [25]. Note that c_i and c_j is normalized before computation. Here we use quadratic term to suppress the background clutters. $w_{ij}^P = e^{-\alpha||p_i - p_j||^2}$ is spatial constrain, which enhances the effect of nearer neighbors. α controls the weight's sensitivity to spatial distance. When $\alpha \to 0$, $w_{ij}^P \to 1$, (2) degrades into global contrast calculation which is similar to that in [10]. In our experiment, we find 5×10^{-5} is suitable for α.

Besides the color contrast, we also introduce the color distribution prior, which meets character (ii) mentioned in Section 1 and is not considered in [10] and [11]. After combining the distribution prior of region R_i, (2) should be rewritten as

$$S_i^{contrast} = D^{prior}(p_i) \sum_j D(c_i, c_j)^2 w_{ij}^P \tag{3}$$

In (3), $D^{prior}(p_i)$ is the distribution prior at position p_i. An advantage of using distribution prior is that we can filter out the background color components which have the similar or even higher contrast than the color components that belong to the real salient object. Notice that in Fig.3, compared with color contrast based methods HC and RC, our approach renders the white road in the background much lower saliency.

According to the fact that human fixation has much higher probability to fall onto the center of the image, $D^{prior}(p_i)$ is larger when p_i is closer to the image center. Here a Gaussian distribution like $D^{prior}(p_i) = e^{-w||p_i - c||^2}$ may be used, in which c denotes image center. However, instead of being puzzled by how to adjust parameter w, which controls the probability distribution of salient object's occurrence, a simple but effective statistical approach is used. We compute the average of 1000 ground truth images[1] provided by [1] (Fig.2), noting that ground truth images are first resized to resolution 400×400. The average image commonly shows where a salient object is most likely to appear. Then it is normalized to have maximum value 1 to form the distribution prior map. In our implementation, the distribution prior map (resolution 400×400) is resized to the input resolution when it is used, and $D^{prior}(p_i)$ is directly obtained from the resized distribution prior map (Fig.2).

Combining color contrast and distribution prior may highlight some parts of an object, leading to the overall object being ambiguous, as is shown in Fig.3.

[1] Actually when we compute the saliency map of an image from this dataset, we should consider the other 999 images' ground truth to calculate the distribution prior. However, the average of 999 images is almost equal to that of 1000 images.

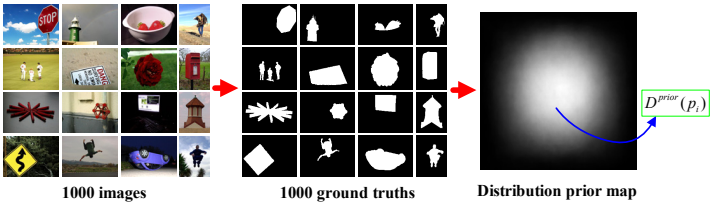

Fig. 2. An illustration for obtaining distribution prior map

The color contrast saliency maps produced by RC [10] and SF (called uniqueness in [11]) also have such problem. As a solution, we adopt saliency smoothing in color space to render regions with similar colors the closer saliency values as

$$\overline{S_i^{contrast}} = \sum_j S_j^{contrast} w_{ij}^C \tag{4}$$

where $\overline{S_i^{contrast}}$ represents the smoothed saliency. $w_{ij}^C = \frac{1}{N^C} e^{-\beta||c_i^{LAB} - c_j^{LAB}||}$ is the weight corresponding to color similarity, as LAB is better for smoothing in practice. $N^C = \sum_j e^{-\beta||c_i^{LAB} - c_j^{LAB}||}$ is its normalization term that guarantees all weights summed to 1. In our experiment, we find that exponent function works better than Gaussians on smoothing saliency of the whole object. In contrast, Gaussians fall down too sharply and usually highlight parts of object. β controls the extent of smoothing. When $\beta \to 0$, $w_{ij}^C \to \frac{1}{N}$, after computing (4), all regions will obtain the same saliency, achieving the most extreme case. When $\beta \to \infty$, output $\overline{S_i^{contrast}}$ equals to $S_i^{contrast}$. Through computing (4), the whole object's saliency becomes more uniform (Fig.3). Here, we set $\beta = 10^{-3}$ for non-normalized LAB color space, which is feasible for highlighting the overall object.

Finally, the smoothed saliency map is normalized to [0, 1] using linear stretch as (5) to get the ultimate color contrast saliency map.

$$\overline{S_i^{contrast}} \leftarrow \frac{\overline{S_i^{contrast}} - \min_j(\overline{S_j^{contrast}})}{\max_j(\overline{S_j^{contrast}}) - \min_j(\overline{S_j^{contrast}})} \tag{5}$$

3.3 Color Distribution

We compute color distribution similarly to [21] to meet character (*iii*), but based on superpixel regions. The distribution of R_i is defined as

$$D_i^{distribution} = ||\sum_j w_{ij}^C p_j^2 - (\sum_j w_{ij}^C p_j)^2||_1 \tag{6}$$

Here, the square of $p_j = (x_j, y_j)^T$ denotes the element square of vector p_j, that is $p_j^2 = (x_j^2, y_j^2)^T$. Actually (6) calculates the distribution variance in x and y direction and uses 1-norm to add them up. High distribution variance indicates that the corresponding color components are widely distributed in the

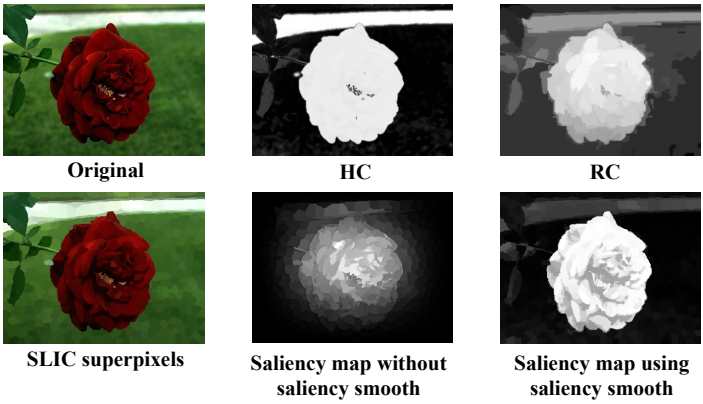

Fig. 3. Our smoothing in color space highlights the overall object. The results of contrast based methods HC and RC are also shown. Notice that the road in the background is rendered the highest saliency by HC while RC highlights the flower unevenly.

whole image and are less likely to belong to a salient object, while low variance indicates a spatially compact distribution.

Note that the parameter β in w_{ij}^C of (6) is tuned differently from that in (4), resulting in more promising performance in practice. In our implementation, β in (6) is set as 10^{-1}. $D_i^{distribution}$ is then normalized to [0, 1] similarly to (5).

As demonstrated above, regions with high distribution variances should obtain low saliency, so we define the color distribution based saliency as

$$S_i^{distribution} = 1 - D_i^{distribution} \tag{7}$$

3.4 Combination and Refinement

We define the final combination as non-linear integration of color distribution saliency and color contrast saliency, as is presented in (8), for we find that such non-linear combination can better pop out salient objects meanwhile suppress background than linear combination.

$$S_i = \overline{S_i^{contrast}} \times S_i^{distribution} \tag{8}$$

After combination, there may still be noises and artifacts due to quantization errors of superpixel segmentation. In order to get high quality saliency maps, we again segment the images into non-compact regions $R'_k, k = 1, 2, 3...N'$ using Mean-shift segmentation [26]. We set fixed parameters $sigmaS = 7, sigmaR = 6.5, minRegion = 240$ for all images. "Non-compact" here means homogenous object surfaces or background will be segmented into one large region. Then the image saliency is refined based on these regions as

$$S_k = \frac{\sum_{I_m \in R'_k} I_m^S}{|R'_k|} \quad s.t.\ I_m^S = S_i|_{I_m \in R_i} \tag{9}$$

where I_m^S is pixel saliency computed by (8). $|R'_k|$ is the sum area of region R'_k. Thanks to this operation, artifacts are eliminated while unconnected parts generated by pre-segmentation become connected. Finally, $S_k, k = 1, 2, 3...N'$ is normalized to [0, 1] to render our final saliency map.

4 Experiment and Comparison

4.1 Visual Comparison

We test our method on the popular public data set provided by [1], which contains 1000 images as well as the corresponding ground truth images. Each image usually contains one unambiguous salient object. We select the current popular 8 state-of-the-art saliency detection methods including IT [9], SR [12], CA [14], FT [1], LC [13], HC [10], RC [10] and SF [11] for comparison. The saliency maps of previous works excluding SF are provided by [10][2]. The SF [11] saliency maps are obtained from the author's webpage[3]. Fig.4 shows several comparison results. Visually, it can be seen that our method obtains relatively higher quality saliency maps compared with the rest 8 methods, which sometimes highlight parts (RC and SF), corners (IT) or edges (SR and CA) with relatively more background clutters (HC, RC, LC and FT). In contrast, our method performs better on stressing out the complete prominent object while suppressing background. The saliency maps of our method for the 1000 images are provided in the supplementary materials.

4.2 Quantitative Comparison

Besides visual comparison, we also implement quantitative comparison. We evaluate the performance of our method by comparing its *precision-recall* rate. For a given threshold T, the *precision* and *recall* rate of a certain saliency detection method are defined as

$$Precision(T) = \frac{1}{1000}\sum_{i=1}^{1000}\frac{|M_i(T) \cap G_i|}{|M_i(T)|},\ Recall(T) = \frac{1}{1000}\sum_{i=1}^{1000}\frac{|M_i(T) \cap G_i|}{|G_i|} \tag{10}$$

where $M_i(T)$ is the binary mask obtained by directly thresholding the saliency map using threshold T on the ith image. G_i is the ground truth. $|\cdot|$ denotes mask's sum area. As we use data set provided by [1], (10) are the averages of 1000 terms. In order to draw the precision and recall curves under different T, we use every possible threshold T from 0 to 255. This is similar to the fixed threshold experiment in [10, 11, 1].

The left two in Fig.5 show the precision and recall curves. As can be seen, our method presents the best precision and recall curve. Our maximum precision

[2] http://cg.cs.tsinghua.edu.cn/people/~cmm/Saliency/Index.htm
[3] http://www.fedeperazzi.com/saliency_filters/

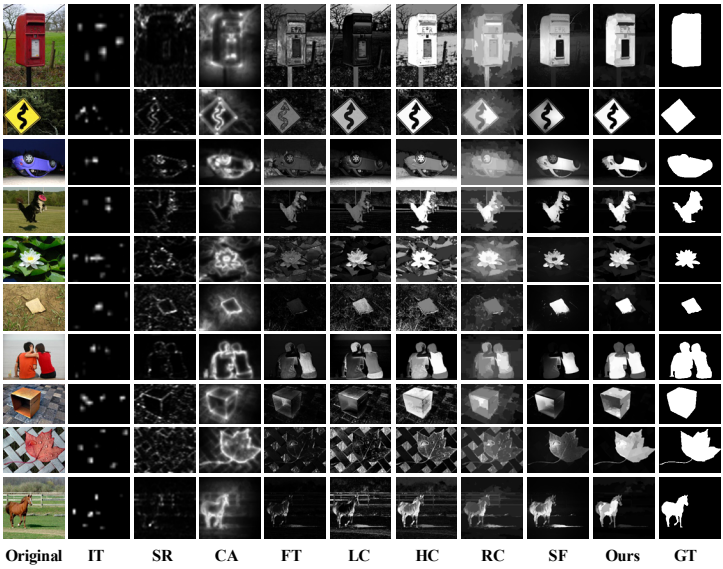

Fig. 4. Visual comparison results between our method and other 8 popular state-of-the-art methods

rate is 96%, with 3% improvement from the second best 93% (SF). Another interesting phenomenon is that our method maintains high precision rate under various recall rate. This is actually consistent with our visual evaluation, which shows our approach provides high quality saliency maps that highlight the whole objects while suppress background, leading to high precision under high recall.

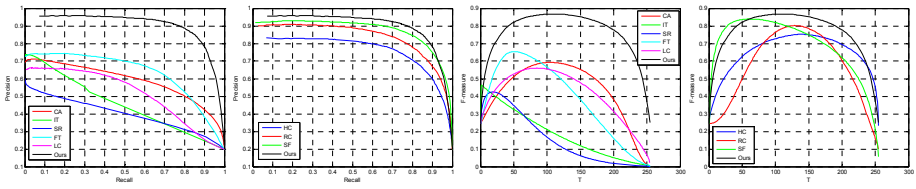

Fig. 5. Precision-recall, F-measure curves of 8 state-of-the-art methods including CA, IT, SR, FT, LC, HC, RC, SF as well as our method

In addition to precision-recall curves, we also evaluate the *F-measure*, which is an integrated evaluation criterion that combines precision and recall as

$$F_\beta(T) = \frac{(1+\beta^2)Precision(T) \times Recall(T)}{\beta^2 \times Precision(T) + Recall(T)} \tag{11}$$

where β^2 is set as 0.3, as is suggested in [10], [11] and [1]. Note that **none of previous works** shows **F-measure curve** varying with threshold T. The

last two in Fig.5 show our F-measure curves. Compare with other methods, our method achieves the best F-measure curve when T varies from 65 to 240 and second best when T varies from 0 to 65. Notice that under this F-measure criterion, RC sometimes performs less better than HC. This may be attributed to that RC achieves higher precision, but lower recall at the same time, which pulls down the F-measure score to some extent. The same thing also happens on SF. As high quality saliency maps can be obtained using our method, using simple fixed threshold can achieve good segmentation results.

Fig.6 presents the evaluation for individual phase of our algorithm, respectively including only contrast, only distribution, without distribution prior, without saliency smoothing and without refinement. It shows the benefit of combining all steps while adding distribution prior and saliency smoothing really works for enhancing the performance.

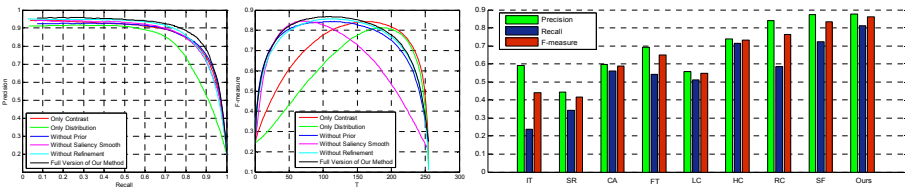

Fig. 6. The first two show the individual phase of our algorithm, respectively including only contrast, only distribution, without distribution prior, without saliency smoothing and without refinement. The last histogram shows the evaluation for adaptive threshold experiment.

Besides, an adaptive threshold experiment, similar to that in [11] and [1], is carried out. The adaptive threshold T_a is defined as two times the mean saliency of an obtained saliency map, as is shown in (12).

$$T_a = \min\{2 \times \frac{\sum_i^M S(I_i)}{M}, T_{max}\} \tag{12}$$

where M denotes the number of pixels in the saliency map and i is pixel index. T_{max} is the upper bound for T_a and is set as 255 by us. The last histogram in Fig.6 shows the precision, recall and F-measure in adaptive threshold experiment. It can be seen that in this experiment, RC still achieves high precision but low recall, because RC usually highlights only part of the real salient object. The precision rate of SF is very close to our method, but our method shows the highest recall rate and F-measure score, respectively 81% (9% improvement) and 0.86 (0.03 improvement).

4.3 Content-Aware Image Resizing

In content-aware image resizing [5–8], saliency maps are usually used to specify relative importance across image parts. Here we use the framework proposed in

[5] to validate the performance of the saliency maps produced by our method on smart image resizing task. The images are scaled along their x-axis. Other cases are straightforward. Fig.7 shows that our method better preserves the whole object than RC and SF during scaling.

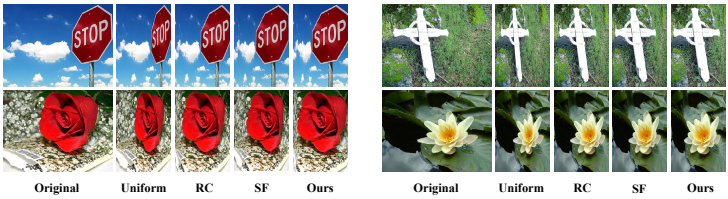

Fig. 7. Using saliency maps of RC, SF and ours on content-aware image resizing

5 Conclusion and Future Work

In this paper, we show how to combine color contrast and distribution to obtain high quality saliency maps, which highlight overall salient object meanwhile suppress the background. Qualitative and quantitative comparisons show that our method outperforms current popular bottom-up saliency detection methods. Our future work includes mining more low-level features which are effective and combining several high-level features like face and human body detection into our system.

Acknowledgement. We thank the anonymous reviewers for their valuable suggestions. This research is partly supported by National Science Foundation, China (No: 61273258).

References

1. Achanta, R., Hemami, S., Estrada, F., Susstrunk, S.: Frequency-tuned salient region detection. In: CVPR (2009)
2. Rutishauser, U., Walther, D., Koch, C., Perona, P.: Is bottom-up attention useful for object recognition? In: CVPR (2004)
3. Han, J., Ngan, K., Li, M., Zhang, H.: Unsupervised extraction of visual attention objects in color images. IEEE TCSV 16, 141–145 (2006)
4. Chen, T., Cheng, M., Tan, P., Shamir, A., Hu, S.: Sketch2photo: Internet image montage. ACM Trans. Graph. 28, 1–10 (2009)
5. Ding, Y., Jing, X., Yu, J.: Importance filtering for image retargeting. In: CVPR (2011)
6. Pritch, Y., Kav-Venaki, E., Peleg, S.: Shift-map image editing. In: ICCV (2009)
7. Grundmann, M., Kwatra, V., Han, M., Essa, I.: Discontinuous seam carving for video retargeting. In: CVPR (2010)
8. Wolf, L., Guttmann, M., Cohen-Or, D.: Non-homogeneous content driven video-retargeting. In: ICCV (2007)

9. Itti, L., Koch, C., NieBur, E.: A model of saliency-based visual attention for rapid scene analysis. IEEE TPAMI 20, 1254–1259 (1998)
10. Cheng, M., Zhang, G., Mitra, N., Huang, X., Hu, S.: Global contrast based salient region detection. In: CVPR (2011)
11. Perazzi, F., Krahenbul, P., Pritch, Y., Hornung, A.: Saliency filters: Contrast based filtering for salient region detection. In: CVPR (2012)
12. Hou, X., Zhang, L.: Saliency detection: A spectral residual approach. In: CVPR (2007)
13. Zhai, Y., Shah, M.: Visual attention detection in video sequences using spatiotemporal cues. ACM Multimedia, 815–824 (2006)
14. Goferman, S., Zelnik-Manor, L., Tal, A.: Context-aware saliency detection. In: CVPR (2010)
15. Parkhurst, D., Law, K., Niebur, E.: Modeling the role of salience in the allocation of overt visual attention. Vision Res. 42, 107–123 (2002)
16. Einhauser, W., Konig, P.: Does luminance-contrast contribute to a saliency map for overt visual attention? Eur. J. Neurosci. 17, 1089–1097 (2003)
17. Fergus, R., Perona, P., Zisserman, A.: Object class recognition by unsupervised scale-invariant learning. In: CVPR (2003)
18. Parikh, D., Zitnick, C.L., Chen, T.: Determining Patch Saliency Using Low-Level Context. In: Forsyth, D., Torr, P., Zisserman, A. (eds.) ECCV 2008, Part II. LNCS, vol. 5303, pp. 446–459. Springer, Heidelberg (2008)
19. Judd, T., Ehinger, K., Durand, F., Torralba, A.: Learning to predict where humans look. In: ICCV (2009)
20. Rother, C., Kolmogorov, V., Blake, A.: Grabcut- interactive foreground extraction using iterated graph cuts. ACM Trans. Graph. 23, 309–314 (2004)
21. Liu, T., Yuan, Z., Sun, J., Wang, J., Zheng, N.: Learning to detect a salient object. IEEE TPAMI 33, 353–367 (2011)
22. Alexe, B., Deselaers, T., Ferrari, V.: What is an object? In: CVPR (2010)
23. Feng, J., Wei, Y., Tao, L., Zhang, C., Sun, J.: Salient object detection by composition. In: ICCV (2011)
24. Achanta, R., Shaji, A., Smith, K., Lucchi, A., Fua, P., Ssstrunk, S.: Slic superpixels. In: Technical report (2010)
25. Borji, A., Itti, L.: Exploiting local and global patch rarities for saliency detection. In: CVPR (2012)
26. Christoudias, C., Georgescu, B., Meer, P.: Synergism in low level vision. In: ICPR (2002)